

Yield Stress Discontinuity in a Simple Glass

F. Varnik¹, O. Henrich²

¹Max-Planck Institut für Eisenforschung, Max-Planck Straße 1, 40237 Düsseldorf, Germany

²Fachbereich für Physik, Universität Konstanz, 78457 Konstanz, Germany

(Dated: October 2, 2018)

Large scale molecular dynamics simulations are performed to study the steady state yielding dynamics of a well established simple glass. In contrast to the supercooled state, where the shear stress, σ , tends to zero at vanishing shear rate, $\dot{\gamma}$, a stress plateau forms in the glass which extends over about two decades in shear rate. This strongly suggests the existence of a finite dynamic yield stress in the glass, $\sigma^+(T) \equiv \sigma(T; \dot{\gamma} \rightarrow 0) > 0$. Furthermore, the temperature dependence of σ^+ suggests a yield stress discontinuity at the glass transition in agreement with recent theoretical predictions. We scrutinize and support this observation by testing explicitly for the assumptions (affine flow, absence of flow induced ordering) inherent in the theory. Also, a qualitative change of the flow curves enables us to bracket the glass transition temperature T_c of the theory from above and (for the first time in simulations) *from below*. Furthermore, the structural relaxation time in the steady state behaves quite similar to the system viscosity at all studied shear rates and temperatures.

PACS numbers: 64.70.Pf, 05.70.Ln, 83.60.Df, 83.60.Fg

Soft glassy materials under shear exhibit a rich phenomenology. In the dilute regime, at temperatures corresponding to the liquid state, forced Rayleigh scattering experiments [1] show an increase of diffusion constant upon shearing (shear thinning), distinct from Taylor dispersion (displacement of particles in the flow direction (x) as they move in the direction of shear gradient. This would give rise to $\langle \Delta x^2(t) \rangle \sim t^3$! [2]. At higher densities, experiments show evidence for shear thinning due to the presence of freely slipping two dimensional crystalline layers [3].

On the other hand, studies of disordered suspensions of hard spheres show that shear thinning and shear melting phenomena may also occur in the absence of a crystalline structure [4]. Similar observations have also been made in light scattering echo studies of (disordered) dense emulsions [5]. Brownian dynamics simulations show that shear thinning in concentrated colloidal suspensions is related to the fact that, in the limit of low shear rates, the main contribution to the shear stress originates from the Brownian motion of colloidal particles and that this contribution decreases with shear rate $\dot{\gamma}$ [6].

Recent theoretical progress, connecting nonlinear rheology with glass formation, prompts us to study in detail by simulations the stationary states of a well established glass model [7] under shear. We focus on the yielding behavior for constant shear rate of glassy states close to but also far below the glass transition temperature.

Recently, Berthier, Barrat and Kurchan studied numerically a driven spin glass and showed that shear thinning can be understood in terms of an acceleration of inherently slow system dynamics by the external drive [8]. Within this approach, the stress depends on the shear rate via a power law (no dynamical yield stress). The 'soft glassy rheology model' of Sollich et al. [9] extends the minimal 'trap model' originally introduced by Bouchaud [10] in order to take into account the effect

of an external drive. The theory contains a noise temperature, x , which controls the distance from the glass transition at $x = 1$. For $1 < x < 2$, a power law decrease of the stress with applied shear rate is found, whereas in the jammed state ($x < 1$), a continuous onset of a dynamic yield stress is predicted, $\sigma^+ \equiv \sigma(\dot{\gamma} \rightarrow 0) = 1 - x$. Fuchs and Cates [11], on the other hand, started from the well studied mode coupling theory (MCT) of the glass transition [12]. They started from the idealized picture that, in a supercooled liquid, nearest neighbors of a particle form a cage which progressively solidifies eventually leading to a complete arrest of all particles as the glass transition is reached. The effect of shear then enters by the advection of density fluctuations. Fluctuations of a given length scale are advected towards progressively shorter length scales so that particles need explore smaller regions in order for density correlations to decay. The interesting prediction of a yield stress discontinuity at the ideal glass transition was made. A related MCT approach to the fluctuations around the steady state has recently been proposed by Miyazaki and Reichman [13]. The issue of yield stress discontinuity, however, could not be addressed in that approach.

Berthier and Barrat [8] performed molecular dynamics simulation studies of the present model under a homogeneous shear showing e.g. that, in a range of low shear rates, time-shear superposition and space time factorization theorems hold thus suggesting that generic properties related to the glass transition 'generalize' to the non-equilibrium situation of a homogeneous shear. However, due to a rather limited range of shear rates, results presented in Ref. [8] did not allow a clear answer whether the present model exhibits a yield stress or not.

In this paper, we focus exactly on this aspect, namely an analysis of the dynamic yield stress and its behavior at the ideal glass transition. For this purpose, we performed large scale molecular dynamics simulations of a generic

glass forming system first introduced by Kob and Andersen [7]. The model consists of a 80:20 binary mixture of Lennard-Jones particles (whose types we call A and B) at a constant total density. A and B particles interact via a Lennard-Jones potential. Standard (dimensionless) parameters will be used as in Refs. [7, 8].

Ten independent samples, equilibrated at a temperature of $T = 0.45$, serve as starting configurations for all simulations reported here. The temperature is set to the desired value at the beginning of shear motion. The shear stress is computed using particle positions and velocities via the Irving-Kirkwood formula [15]. Only samples corresponding to the steady state, i.e. to strains larger than 100%, are taken into account (previous studies of the stress-strain relation of the same model showed that the initial transient behavior is limited to strains below 50% [14]). Depending on the desired accuracy of the stress-data, the length of simulations was varied between 380% and 760% strain. Equations of motion are integrated using a discrete time step of $dt = 0.005$.

Recently, it was found that the present model may exhibit shear-localization in the glassy state if the shear rate is imposed by using a conventional Couette cell with moving atomistic walls [14]. In the present analysis, however, we are interested in effects of a spatially constant shear rate, a basic ingredient of all theories briefly addressed above. Therefore, we do not use atomistic walls but apply the so called SLLOD algorithm combined with Lees-Edwards boundary condition [15]. With this simulation method, we do indeed observe a linear velocity profile in all studied cases (not shown).

As shear may, at least in principle, change the static structure of the system, we examine this by computing pair distribution functions along x (flow), y and z (shear gradient) directions separately. Figure 1 illustrates results on $g(x)$, $g(y)$ and $g(z)$ (A-A correlations) for three characteristic temperatures $T = 0.2$ (deep in the glass), $T = 0.42$ (close to T_c) and $T = 0.6$ (supercooled state) indicating the absence of long range order in all studied cases. Surprisingly, even though the stress changes

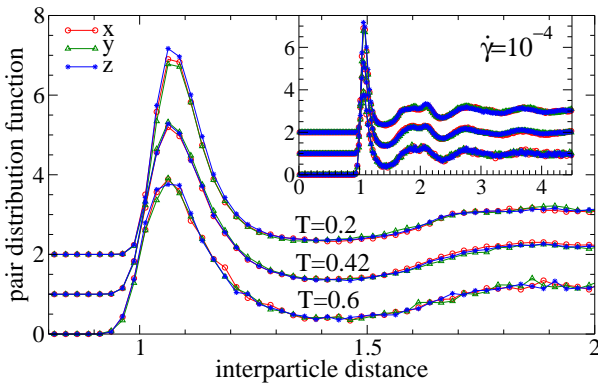


FIG. 1: A-A pair correlation functions along x (flow), y and z (shear gradient) directions, for three characteristic temperatures: $T = 0.2$ (glass), $T = 0.42$ (close to T_c) and $T = 0.6$ (supercooled state). The shear rate is $\dot{\gamma} = 10^{-4}$. For clarity, data at $T = 0.42$ ($T = 0.2$) are shifted upwards by 1 (2).

by more than a decade at this $\dot{\gamma}$, the local structure varies little with shear, remains amorphous, and (almost) isotropic. Similar observations are also made using the B-B and A-B pair correlations.

Figure 2 shows simulated steady state shear stresses as functions of shear rate (viz. 'flow curves') for temperatures ranging from far above to far below the glass transition temperature of the model. Note that shearing allows us to access stationary states at very low temperatures. As apparent from the change of the curvature of the flow curves (S-shaped without extended horizontal piece at high, horizontal piece merging into upward curvature at low temperatures) the system response changes qualitatively around a temperature T_c , which MCT identifies as (ideal) glass transition temperature. For $T > T_c$ the stress becomes proportional to shear rate as $\dot{\gamma}$ approaches zero (linear response). At temperatures below T_c , however, a stress plateau forms in the low $\dot{\gamma}$ -regime. The observed qualitative agreement with the MCT scenario prompts us to test its predictions in more detail. Importantly, the qualitative change manifest in the $\sigma(\dot{\gamma})$ curves enables us to give upper and lower limits for T_c without any theoretical analysis: we conclude $0.34 < T_c < 0.45$. Fits with the schematic $F_{12}^{\dot{\gamma}}$ -model of MCT support this estimate, and achieve to describe the flow curves for *all* studied temperatures by adjusting two global parameters (a scale for $\dot{\gamma}$ and one for σ), and the parameter ε at each temperature measuring the distance to the ideal glass transition [16]. The fit gives $T_c = 0.4$ and $\sigma_{c,th}^+ = 0.19$. We thus conclude that the basic rheological features of our model are well described within simple schematic models in the framework of the idealized MCT. Relaxation channels not contained in the idealized MCT (so-called 'hopping effects' [7], which may be the origin for the deviations from theory at very low $\dot{\gamma}$ in Fig. 2) can not falsify our bound for T_c , because the qualitatively different shapes of the flow curves are the characteristics of the fluid or glassy states within MCT.

The stress plateau is best developed for tempera-

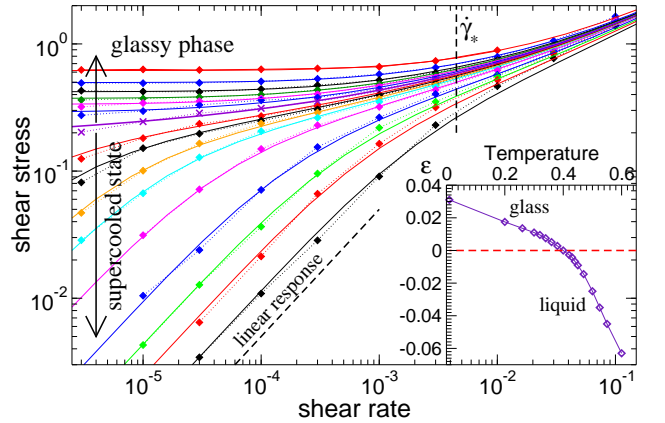


FIG. 2: Simulated shear stress (symbols) compared to theoretical predictions (solid lines) for various temperatures ($T = 0.01$ to $T = 0.60$ from top to bottom). The inset shows the fitted separation parameter, ε , versus T .

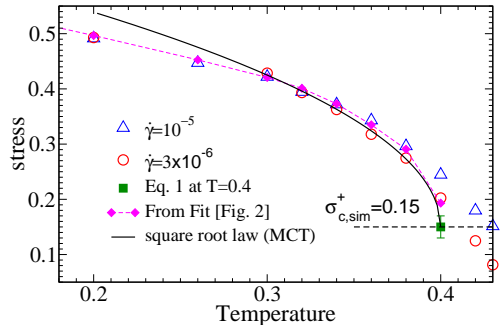


FIG. 3: Determination of dynamic yield stress and its temperature dependence (see text).

tures deep in the glassy phase extending over about two decades in shear rate. Its onset is shifted toward progressively lower $\dot{\gamma}$ as the temperature is increased toward T_c . This makes an estimate of the dynamic yield stress, $\sigma^+(T) \equiv \sigma(T; \dot{\gamma} \rightarrow 0)$, a difficult task for temperatures below but close to T_c . Nevertheless, an estimate of $\sigma^+(T)$ is interesting because it highlights the anomalous weakening of the glass when heating to T_c . Testing the MCT predictions below T_c has previously not been possible in simulations because of problems to reach the equilibrated or steady state at sufficiently low shear rates. Our estimate is obtained by comparing the steady state shear stress for the two lowest simulated shear rates, namely $\dot{\gamma} = 10^{-5}$ and $\dot{\gamma} = 3 \times 10^{-6}$. As shown in Fig. 3, at temperatures below $T = 0.38$, practically the same shear stress is obtained for both choices of $\dot{\gamma}$ indicating the presence of a yield stress plateau.

For $T = T_c$, we make use of theoretical predictions based on the F_{12}^γ -model [16]. For not too low shear rates, the flow curve takes the form of a generalized Herschel-Bulkeley constitutive equation,

$$\sigma = \sigma_c^+ (1 + |\dot{\gamma}/\dot{\gamma}_*|^m + c_2 |\dot{\gamma}/\dot{\gamma}_*|^{2m} + c_3 |\dot{\gamma}/\dot{\gamma}_*|^{3m}). \quad (1)$$

Here, $\dot{\gamma}_*$ is an upper limit where this expansion holds. As the simple F_{12}^γ -model is found to describe the rheological properties of our system rather well (see the discussion of Fig. 2), we set the parameters, $c_2 = 0.896$, $c_3 = 0.95$ and $m = 0.143$ as obtained from an analysis of the model [16]. We then apply a fit to Eq. 1 with σ_c^+ and $\dot{\gamma}_*$ being the only fit parameters. This gives $\sigma_c^+ = 0.15 \pm 0.01$ and $\dot{\gamma}_* = 0.0045 \pm 0.0008$ the latter being close to our estimate of the window, where MCT can describe the flow curves. At higher shear rates, $\dot{\gamma} > \dot{\gamma}_*$, we expect microscopic effects to dominate the stress. As shown in Fig. 3, while $\sigma^+(T)$ weakly varies with T at low temperatures, it steeply drops as T approaches T_c , signalling the glass transition. The yield stress follows well the MCT-square root law [11], $\sigma^+(T) - \sigma_c^+ \propto |1 - T/T_c|^{0.5}$.

Note that the critical temperature of $T_c = 0.4$, used in order to obtain best agreement between the theory and simulations, is slightly lower than the estimate $T_c = 0.435$ obtained from the analysis of the equilibrium dynamics of the system [7]. This discrepancy is possibly related

to the hopping effects observed in the density correlation functions closely above T_c [7, 17]. A closer analysis of this aspect requires understanding of hopping effects under shear and is beyond the scope of the present report.

Next we address the close connection between observed non-linearity in the flow curves and the structural relaxation as reflected in the incoherent scattering function, $\Phi_q(t) = \langle \sum_{i=1}^{N_A} \exp[q_y(y_i(t) - y_i(0))] \rangle / N_A$. Here, N_A is the number of A-particles, q_y is the y -component of the wave vector and y_i is the y -component of the position of i -th particle. We set $q_y = 7.1$ to the inverse of the average interparticle distance (or, equivalently, the maximum position of the static structure factor). The above definition of $\Phi_q(t)$ takes into account the fact that the imposed flow is in the x -direction and the shear gradient in the z -direction, and eliminates the advection of particles with the flow. Note that the above choice of A type is arbitrary. Similar results are also obtained for type B particles (not shown).

Figure 4 illustrates $\Phi_q(t)$ for $T = 0.3$ (glass) for all studied shear rates. First, $\Phi_q(t)$ exhibits the two step relaxation process typical of supercooled liquids: A short time decay to a plateau, f_q (characterizing the 'solidity' of the system at length scale $1/q$ [12]) followed by a final decay to zero at much larger times. The long time decay of $\Phi_q(t)$, on the other hand, is clearly dominated by the imposed shear. Its shape does not depend on the shear rate which only sets the time scale, $\tau_q \sim 1/\dot{\gamma}$. Note that Fig. 4, and the stationarity of the correlators, verifies that we achieved ergodic stationary states as expected from theory.

Figure 5 depicts $\hat{\sigma} = \tau_q \dot{\gamma}$ (this definition of a stress goes back to Maxwell) for $q = 7.1$ versus $\dot{\gamma}$ for various temperatures. Here, $\tau_q = \int_0^\infty dt \Phi_q(t)$ is defined as average relaxation time. Where $\tau_q \sim 1/\dot{\gamma}$ holds, a plateau in $\hat{\sigma}$ follows. Note the striking similarity between the $\dot{\gamma}$ -dependence of the shear stress (σ ; Fig. 2) and that of $\hat{\sigma}$. As suggested by the inset of Fig. 5, in the whole range of studied shear rates and temperatures, $\hat{\sigma}/\sigma$ changes at most by a factor of two whereas the shear stress varies by two orders of magnitude. Thus, both the $\dot{\gamma}$ and T -

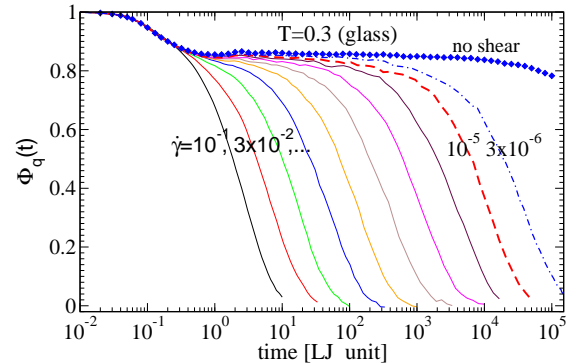


FIG. 4: Steady state incoherent scattering function, $\Phi_q(t)$, of a glass ($T = 0.3$) measured at various shear rates as indicated, and for $q = 7.1$. The quiescent $\Phi_q(\dot{\gamma} = 0)$ after a waiting time of $t_w = 10^5$ is also shown.

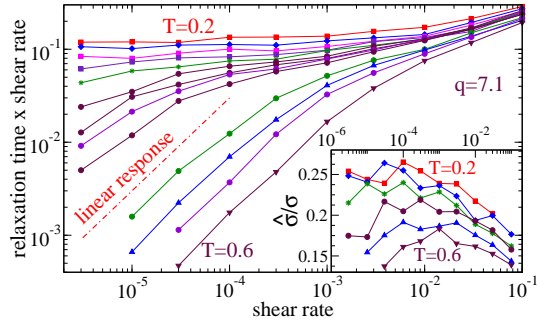


FIG. 5: $\hat{\sigma} \equiv \tau_q \dot{\gamma}$ versus shear rate for various temperatures ranging from the glassy phase to the supercooled state. The inset shows the ratio of this (Maxwell type) stress to the real shear stress for $T = 0.2, 0.3, 0.4, 0.45, 0.525$ and 0.6 .

dependence of steady state shear stress is mainly determined by that of $\hat{\sigma} = \dot{\gamma} \tau_q$. This observation is quite significant as it supports theoretical approaches where, even beyond the Newtonian-regime, the shear viscosity is simply taken as a relaxation time [8, 13], or where this relation holds as approximation [11].

In summary, large scale molecular dynamics simulations have been performed in order to investigate the existence and temperature dependence of the dynamic yield stress, σ^+ , for a 80:20 binary Lennard-Jones model glass first proposed by Kob and Andersen [7]. Our data do indeed support the existence of a dynamic yield stress in

the glassy phase as underlined by stress plateaus extending over about two decades in shear rate. Let us mention recent experiments on the rheology of dense colloidal dispersions [18] which also find finite σ^+ . Furthermore, the temperature dependence of σ^+ follows the predicted anomalous weakening close to the glass transition with a finite critical yield stress of $\sigma_c^+ = 0.17 \pm 0.02$ as a compromise between $\sigma_{c,\text{th}}^+ = 0.19$ and $\sigma_{c,\text{sim}}^+ = 0.15$. The flow curves allow for the first bracketing in simulations of the critical temperature of MCT *from below*. Irrespective of hopping effects neglected in the employed MCT, we can conclude $T_c > 0.34$.

Furthermore, a generalized stress ($\hat{\sigma}$; Fig. 5) as the product of the shear rate and the structural relaxation time was determined for all temperatures and shear rates. $\hat{\sigma}$ exhibits exactly the same qualitative features as the real shear stress thus emphasizing the close connection between the structural relaxation and the rheological response. Noting that *a priori* no relation $\hat{\sigma}$ to σ exists [11], this finding corroborates theoretical approaches which make use of the relaxation time as a sort of viscosity.

Acknowledgments

We thank J.-L. Barrat, L. Berthier, L. Bocquet, M. E. Cates and J. Horbach for useful discussions. F.V. was supported by the DFG, Grant No VA 205/1-1, and O.H. by the DFG IGC 'Soft Matter'. Simulation time was granted by the ZDV-Mainz and PSMN-Lyon and IDRIS (project No 031668-CP: 9).

[1] X. Qiu, H. Ou-Yang, D. Pine, and P. Chaikin, Phys. Rev. Lett. **61**, 2554 (1988).

[2] G. Taylor, Proc. R. Soc. London A **219**, 186 (1953).

[3] B. Ackerson and N. Clark, Phys. Rev. Lett. **46**, 123 (1981); B. Ackerson, J. Rheol **34**, 553 (1990).

[4] G. Petekidis *et al.*, Physica A **306**, 334 (2002); A. M. G. Petekidis and P. Pusey, Phys. Rev. E **66**, 051402 (2002); G. Petekidis, D. Vlassopoulos, and P. Pusey, Faraday Discuss. **123**, 287 (1999); H. M. Laun, R. Bung, S. Hess, W. Loose, O. Hess, K. Hahn, E. Hädicke, R. Hingmann, F. Schmidt, and P. Lindner, J. Rheology **36**, 743 (1992).

[5] P. Hébraud, F. Lequeux, J. Munch, and D. Pine, Phys. Rev. Lett. **78**, 4657 (1997).

[6] T. Phung, J. Brady, and G. Bossis, J. Fluid Mech. **313**, 181 (1996); P. Strating Phys. Rev. E **59** 2175 (1999).

[7] W. Kob and H. C. Andersen, Phys. Rev. Lett. **73**, 1376 (1994). W. Kob and H. C. Andersen, Phys. Rev. E **51**, 4626 (1995); *ibid* **52**, 4134 (1995).

[8] L. Berthier, J.-L. Barrat, and J. Kurchan, Phys. Rev. E **61**, 5464 (2000); L. Berthier and J.-L. Barrat, J. Chem. Phys. **116**, 6228 (2002); L. Berthier, J. Phys.: Condens. Matter **15**, S933 (2003).

[9] P. Sollich, F. Lequeux, P. Hébraud and M.E. Cates, Phys. Rev. Lett. **78**, 2020 (1997), P. Sollich, Phys. Rev. E **58**, 738 (1998).

[10] J. Bouchaud, J. Phys. I **2**, 1705 (1992).

[11] M. Fuchs and M. E. Cates, Phys. Rev. Lett. **89**, 248304 (2002); M. Fuchs and M. E. Cates, Faraday Discuss. **123**, 267 (2003); M. Fuchs and M. E. Cates, J. Phys. Condens. Matter (**17** S1681, 2005).

[12] W. Götze, in *Les Houches 1989, Session LI*, edited by J. P. Hansen, D. Levesque, and J. Zinn-Justin (North-Holland, Amsterdam, 1989), pp. 287–503.

[13] K. Miyazaki and D. Reichman, Phys. Rev. E **66**, 050501 (2002); K. Miyazaki, D. Reichman, and R. Yamamoto, Phys. Rev. E **70**, 011501 (2004).

[14] F. Varnik, L. Bocquet, J.-L. Barrat, and L. Berthier, Phys. Rev. Lett. **90**, 095702 (2003); F. Varnik, L. Bocquet and J.-L. Barrat J. Chem. Phys. **120**, 2788 (2004).

[15] D. J. Evans and G. P. Morriss, *Statistical Mechanics of Non Equilibrium Liquids* (Academic Press, London, 1990).

[16] O. Henrich, F. Varnik, and M. Fuchs J.Phys.: Condens. Matter **17**, 1 2005.

[17] E. Flenner, and G. Szamel, Phys. Rev. E **72**, 011205 (2005).

[18] G. Petekidis, D. Vlassopoulos, and P.N. Pusey, J.Phys.: Condens. matter **16**, S3955 (2004); M. Fuchs and M. Ballauff, J. Chem. Phys. **122**, 094707 2005.